

The interplay between upwelling and deep convective mixing in determining the seasonal phytoplankton dynamics in the Gulf of Aqaba: Evidence from SeaWiFS and MODIS

Rochelle G. Labiosa¹ and Kevin R. Arrigo

Ocean Biogeochemistry Lab, Department of Geophysics, Stanford University, Stanford, California 94305-2215

Amatzia Genin

The Interuniversity Institute for Marine Sciences, POB 469, Eilat 88103, Israel

Stephen G. Monismith

Department of Civil and Environmental Engineering, Stanford University, Stanford, California 94305

Gert van Dijken

Ocean Biogeochemistry Lab, Department of Geophysics, Stanford University, Stanford, California 94305-2215

Abstract

In the Gulf of Aqaba, the northeasternmost segment of the Red Sea, phytoplankton blooms are more intense than in other oligotrophic regions (e.g., the Sargasso Sea). In this study, we use multiyear in situ (1988–2000) and SeaWiFS (1999–2001) chlorophyll *a* (Chl *a*) data to describe the dynamics of phytoplankton biomass throughout the Gulf of Aqaba. The temporal pattern of phytoplankton biomass in the Gulf of Aqaba includes a strong spring bloom and a somewhat weaker autumn bloom, the length, intensity, and timing of which vary from year to year. In addition, highly positive west-to-east (W to E) gradients in Chl *a* were found throughout the Gulf of Aqaba. A corresponding negative gradient in sea surface temperature (SST) obtained from MODerate resolution Imaging Spectroradiometer (MODIS) in 2001 indicates that the gradient of Chl *a* across the Gulf of Aqaba is an outcome of an Ekman-driven upwelling along the eastern side. Calculations of the upwelling and convective fluxes that are based on meteorological data from Eilat, Israel, indicate that upwelling is comparable to or exceeds convection during much of the year. We present a conceptual model demonstrating how upwelling and convection can either support or oppose each other, thereby jointly controlling mixed-layer depth and the development of phytoplankton blooms. Coastal upwelling plays a larger role in controlling phytoplankton dynamics than was previously thought, and it explains much of the observed spatial and temporal variability in phytoplankton distributions.

The Gulf of Aqaba, located off the northern Red Sea (Fig. 1), has been called an oligotrophic sea (e.g., Levanon-Spanier et al. 1979; Reiss and Hottinger 1984), but unlike other oligotrophic subtropical seas (e.g., Ondrusek et al. 1991; Letelier et al. 1996; Marañon et al. 2000), it undergoes marked seasonal fluctuations in both phytoplankton biomass and primary production (Genin et al. 1995; Lindell and Post 1995). In early fall, a negative heat flux at the ocean–atmosphere interface causes sea surface cooling. The cooled surface wa-

ter convectively mixes to depth, creating a deeply mixed surface layer, thus bringing nutrients to the surface (Wolf-Vecht et al. 1992; Genin et al. 1995). Mixing depth is maximal in late winter, with the degree of mixing dependent on the amount of atmospheric cooling during the preceding winter. Typically, convective mixing reaches to about 300 m, while mixing depths of 860 m were measured during the unusually cold winter of 1992 (Genin et al. 1995).

In early spring, a phytoplankton bloom usually develops after air temperatures warm and surface waters begin to stratify, increasing the average exposure of phytoplankton to light. The majority of phytoplankton (>95%) in the Gulf of Aqaba are ultraphytoplankton (<8 μm) (Lindell and Post 1995; Post et al. 1996), including *Synechococcus*, *Prochlorococcus* (Lindell and Post 1995; Post et al. 1996; Li et al. 1998; Sommer et al. 2002), and small eukaryotes, comparable to classic oligotrophic regions. However, unlike some oligotrophic regions (e.g., Claustre and Marty 1995), the phytoplankton community structure exhibits strong seasonality, with *Synechococcus* and *Prochlorococcus* dominating during the spring and summer, respectively, and eukaryotic phytoplankton (specifically dinoflagellates and diatoms) dominating during winter (Reiss and Hottinger 1984; Lindell

¹ Corresponding author (jahajey@pangea.stanford.edu).

Acknowledgments

We thank the Israel Meteorological Service for the wind, air temperature, and radiation data from Eilat. R.G.L. would like to thank Tasha Reddy for her technical assistance. We also thank André Morel and two anonymous reviewers for their helpful comments and suggestions.

This work has been funded by the NASA Earth Systems Science fellowship program (ESS/01-000-0234) to R.G.L. The field work in the Gulf of Aqaba was funded by grant 1997450 from the U.S./Israel Binational Science Foundation (BSF) to A.G. and S.M. and a grant from the USAID through the Red Sea Marine Peace Park, a joint Jordanian–Israeli program.

resolution Chl *a* imagery for the Gulf of Aqaba were recorded between 1999 and 2001 by three High-Resolution Picture Transmission (HRPT) stations and distributed through NASA's Goddard Distributed Active Archive Center (DAAC). Data for 1997 and 1998 are relatively scarce because of a paucity of HRPT collection stations in the region at that time. The Level 1 Local Area Coverage images from SeaWiFS were processed using the NASA SeaWiFS Data Analysis System (SeaDAS) image processing software with the OC4v4 algorithm and then mapped using a cylindrical projection. Slightly less than one full yr of MODIS 1-km resolution SST imagery was available directly from the DAAC. The MODIS Level 2 SST data were filtered to quality levels of 0 and 1 (first and second best-quality pixels, suggested for coastal areas) and mapped to the same projection with Interactive Data Language (Research Systems) scripts written for SeaDAS. Temporal resolution provided by the images was generally one cloud-free image every 3 d for both SST and Chl *a*, but because of infrequent high-resolution satellite data collection by the HRPT stations during some months, this number was at times as few as two per month.

Once the images were processed to level 3, all images of low quality (e.g., distorted pixels at the edge of the swath, low data coverage) were discarded from the data set. The processed SeaWiFS images include Level 2 Flags (various indicators of pixel quality), which were also examined, particularly for evidence of turbidity. Turbidity can result in Chl *a* overestimates and atmospheric correction failure, as the atmospheric correction algorithm is compromised by non-zero water leaving radiance at 765 and 865 nm. Because the Gulf of Aqaba is a narrow basin with steeply sloping coastal shelves and little river runoff, turbidity was not prevalent in the images used in this study. Large amounts of dust can also compromise satellite-based estimates of Chl *a* (Claustre et al. 2002). However, this effect usually leads to overestimates compared to low in situ values, the opposite of what we observed in this study.

To quantify horizontal gradients in Chl *a* and SST, three zonal transects (A1, A2, and A3) and one meridional transect (AL) were extracted from all projected satellite images (Fig. 1). The meridional transect allows monitoring of the intrusion of waters from the Red Sea proper and their migration northward in the Gulf of Aqaba and enables comparison between the northern and southern zones of the Gulf. After the Chl *a* and SST data were extracted along the transects using the SeaDAS *r line* script, the data were interpolated linearly in space and time, and individual images were combined to create weekly averages. For the Chl *a* satellite data, we refer to a bloom as a level of Chl *a* greater than twice the average summer value during the 3 yr, $>0.4 \text{ mg m}^{-3}$.

In situ data—In coordination with the Israel Meteorological Service, the H. Steinitz Marine Biology Laboratory at the Interuniversity of Marine Sciences in Eilat, Israel (29.504°N, 34.919°E), maintains a data archive containing local wind speed and direction, air temperature, humidity, and downwelling irradiance. SST and sea surface Chl *a* were measured daily (between 0800 to 1000 h local time) at a nearby pier as described by Genin et al. (1995). The mete-

orological measurements were made with a Met One meteorological station (Campbell Scientific). Chl *a* was measured fluorometrically after filtering the water sample through a GF/F filter and was then cold extracted (5°C) in 90% acetone for 24 h. The in situ data we used consisted of 3 yr of wind data (1999–2001), 13 yr of Chl *a* (1988–2000), and 4 yr of SST (1997–2000). Depth profiles of temperature and conductivity at Sta. A (Fig. 1), made with a conductivity temperature depth profiler (CTD; Applied Microsystems and Seabird), were provided by the Red Sea Marine Peace Park, a Jordanian and Israeli program funded by the U.S. Agency for International Development (USAID) (Zimmer 2001).

All data sets were binned to produce both daily and weekly means. In addition, the 10-min wind direction values were segregated into northerly (upwelling inducing on the east side of the Gulf of Aqaba) and all other directional components to calculate the fraction of each week that the winds were upwelling favorable. Days with invalid data or partial data coverage were eliminated from the analysis, and the remaining days were interpolated linearly to create a complete daily data set. In the absence of in situ nutrient data, wind, air temperature, and SST data were used to calculate the wind-supported Ekman transport of nutrients to the surface of the Gulf of Aqaba.

One way of comparing the relative basinwide importance of convection and upwelling fluxes in the forcing of phytoplankton blooms (i.e., in terms of supplying nutrients from the deep parts of the Gulf of Aqaba to the surface mixed layer) is to compare the fluxes into the surface mixed layer that result from both processes. However, it is important to recognize that they occur in two different ways: upwelling takes the lower layer fluid and first brings it to the surface in the upwelling region and then mixes it laterally (Blanton 1973). In contrast, convective mixing acts more uniformly across the surface of the basin, entraining fluid from below the thermocline and incorporating it locally into the mixed layer. To make this comparison, we first determined the percentage of the time when winds were from the north (upwelling favorable) and computed the Ekman flux for that period as follows. For a given wind stress, the offshore Ekman drift must be equal to the integral over the upwelling region of the vertical flow from depth to the surface (Gill 1982). The Ekman drift (T) was calculated as the wind stress (τ) divided by the Coriolis parameter (f).

$$T = \frac{\tau}{\rho_{\text{water}} f} \cos \theta_{\text{wind}} = \frac{\rho_{\text{air}} (U_{10}^2 C_d)}{\rho_{\text{water}} f} \cos \theta_{\text{wind}} \quad (1)$$

where f is the Coriolis parameter ($7.2 \times 10^{-5} \text{ s}^{-1}$ at 30° latitude), ρ_{air} is the density of air (1.5 kg m^{-3}), ρ_{water} is the density of seawater ($\sim 1,027 \text{ kg m}^{-3}$), U_{10} is the wind speed 10 m above sea level, C_d is the drag coefficient (calculated as $0.44 + 0.000063 \times U_{10}$, Smith 1980), and θ_{wind} is the number of degrees that the wind deviates from the optimal upwelling wind direction (the alongshore direction of 15°). To compare the effects of upwelling and convection, the entrainment velocity computed at the base of the mixed layer was multiplied by the width of the Gulf of Aqaba to compute a total entrainment flux per unit length of the Gulf of Aqaba. Following Sherman et al. (1978), the entrainment velocity

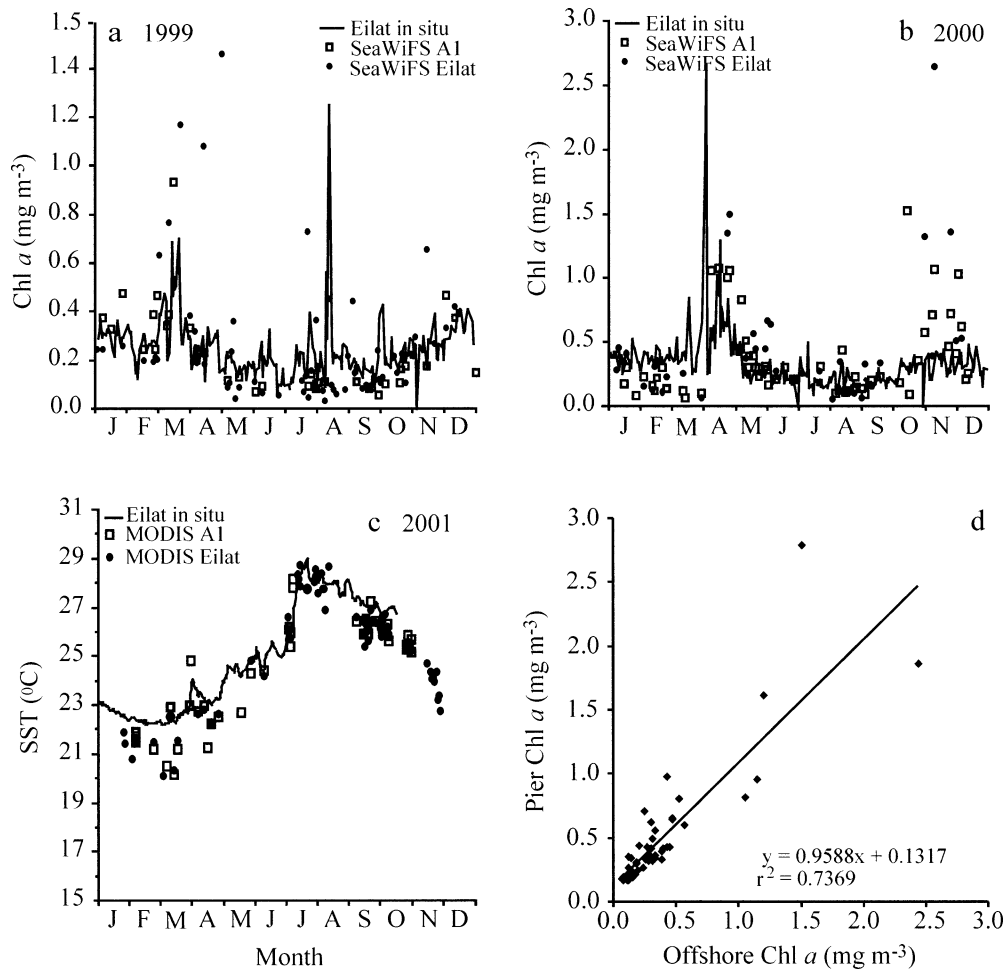


Fig. 2. SeaWiFS Chl *a* data are compared to in situ data from Eilat in (a) 1999 and (b) 2000. (c) MODIS SSTs are compared to in situ Eilat SSTs for 2001. Squares represent the averages of transect A1, and circles represent data from the closest possible point to Eilat (average of 16 pixels). (d) Chl *a* data from Eilat correlated with open-water data (1 km offshore) from the Gulf of Aqaba, $r^2 = 0.74$, 4×4 pixel box.

can be split into two parts: (1) the entrainment due to turbulence produced by both wave breaking and shear at the near-surface layer, and (2) the entrainment due to convective mixing. Generally, the entrainment flux was significant only when it was dominated by convection, conditions that generally were found when the upper mixed layer was deepening and cooling. For these cases, the entrainment velocity, u_e , can be estimated to be as follows:

$$u_e = 0.3 \frac{H_L + H_S + H_{Lw}}{\rho_{\text{water}} C_p \Delta T} \quad (2)$$

where H_L is the latent heat flux, H_S is the sensible heat flux, H_{Lw} is the net longwave radiation, ρ_{water} is the density of water, C_p is the specific heat capacity of water, and ΔT is the difference in temperature between the mixed layer and the water below. This relation assumes that 30% of the cooling flux results in mixing, a reasonable approximation for convective mixing (Sherman et al. 1978).

SeaWiFS Chl a and MODIS SST validation—In situ data were used to validate the SeaWiFS-derived Chl *a* and the

MODIS-derived SST. Because all in situ data are from Eilat, Israel, the satellite data within a 16-pixel box (centered at approximately 29.44°N, 34.92°E, as close as possible to Eilat) as well as along the A1 transect (more valid pixels were available for averaging purposes) were compared to the in situ data after they were temporally averaged using the same weekly bins. The fits between the Gulf of Aqaba satellite data and the in situ data for 1999 and 2000 (Chl *a*) and 2001 (SST) are acceptable (Fig. 2a–c). However, SeaWiFS appears to underestimate slightly the in situ Chl *a* at lower values ($<0.2 \text{ mg m}^{-3}$) and overestimate them at higher values (bloom periods). Similarly, MODIS and Eilat SSTs agree well, although there is a slight underestimation by MODIS at the lower values of SST, probably because of the location offset between the MODIS and Eilat sampling points. Disregarding possible calibration problems, the differences between the remotely sensed and in situ data could be due to several factors, including (1) the lack of coherence between the Eilat sampling days and days for which satellite imagery were available, (2) the larger spatial area included in the remote-sensing averaging (in situ data were taken from one

location in Eilat), and (3) the differences between open-water data values and Eilat values, as none of the remotely sensed data included the Eilat pier. However, the fit between open-water Chl *a* (1 km offshore) and Eilat pier Chl *a* collected during several years is good ($r^2 = 0.74$), although there is more scatter at the higher values (Fig. 2d). On the basis of these comparisons, we believe that the SeaWiFS Chl *a* and MODIS SST algorithms perform well in the Gulf of Aqaba.

Results

*The annual cycle in Chl *a* and SST*—During a typical annual cycle, phytoplankton populations in the Gulf of Aqaba undergo a large bloom in the spring and a smaller bloom in the autumn. The Chl *a* distribution throughout the Gulf of Aqaba exhibits this same annual cycle, except for the southern edge near the Straits of Tiran and the eastern margin of the Gulf of Aqaba (upwelling side when winds are northerly), which are on average >0.5 mg Chl *a* m^{-3} higher than the rest of the Gulf of Aqaba (Fig. 3a). Prebloom Chl *a* concentrations are relatively high in winter, ranging from 0.3 to 0.5 mg m^{-3} . Between March and April, the spring bloom develops and persists for an average of 3 months. Concentrations of Chl *a* associated with this bloom can be as high as 3 mg m^{-3} , but they typically average a more modest 0.8 mg m^{-3} . Zonal transects from the Gulf of Aqaba all show a positive W to E gradient in Chl *a* (Fig. 4a,c) throughout the year, with the gradients being particularly strong during the spring and autumn blooms. Ultimately, nutrients become depleted by phytoplankton in summer, and Chl *a* drops to its lowest levels of the year, averaging 0.2 mg m^{-3} between the end of May and the end of September. By the beginning of October, Chl *a* begins to increase again, as autumn convection commences, eventually attaining wintertime values.

Phytoplankton biomass can change rapidly during the season, with Chl *a* occasionally increasing by an order of magnitude or more within the span of a few days. For example, in the northern Gulf of Aqaba (29.0°N–29.5°N) between 17 March 1999 and 19 March 1999, Chl *a* increased by a factor of >10 , from 0.70 to 7.5 mg m^{-3} (Fig. 5a). Similarly, Chl *a* increased by a factor of 15 within a 2-d period, from 0.26 to 3.9 mg m^{-3} between 16 February 2000 and 18 February 2000 (Fig. 5b). The minimum specific growth rates calculated from such increases in Chl *a* are 1.96 and 1.71 d^{-1} for February 1999 and March 2000, respectively, which are consistent with published nonlimited net growth rates at $>20^{\circ}C$ (Eppley 1972).

In situ data from Eilat for a 12-yr period (Fig. 6a) show that there is considerable interannual variability in the Chl *a* concentrations associated with phytoplankton blooms, including variability in the intensity, length and timing of the blooms. During some years (e.g., 1996 and 1999), the maximum spring Chl *a* levels reached only <1 mg m^{-3} , while during other years (e.g., 1992 and 2000), Chl *a* peaked at >3 mg m^{-3} . Some spring blooms were characterized by a single broad peak in Chl *a* that lasted several months (e.g., >14 weeks in 1992, see Fig. 6a, inset), while others con-

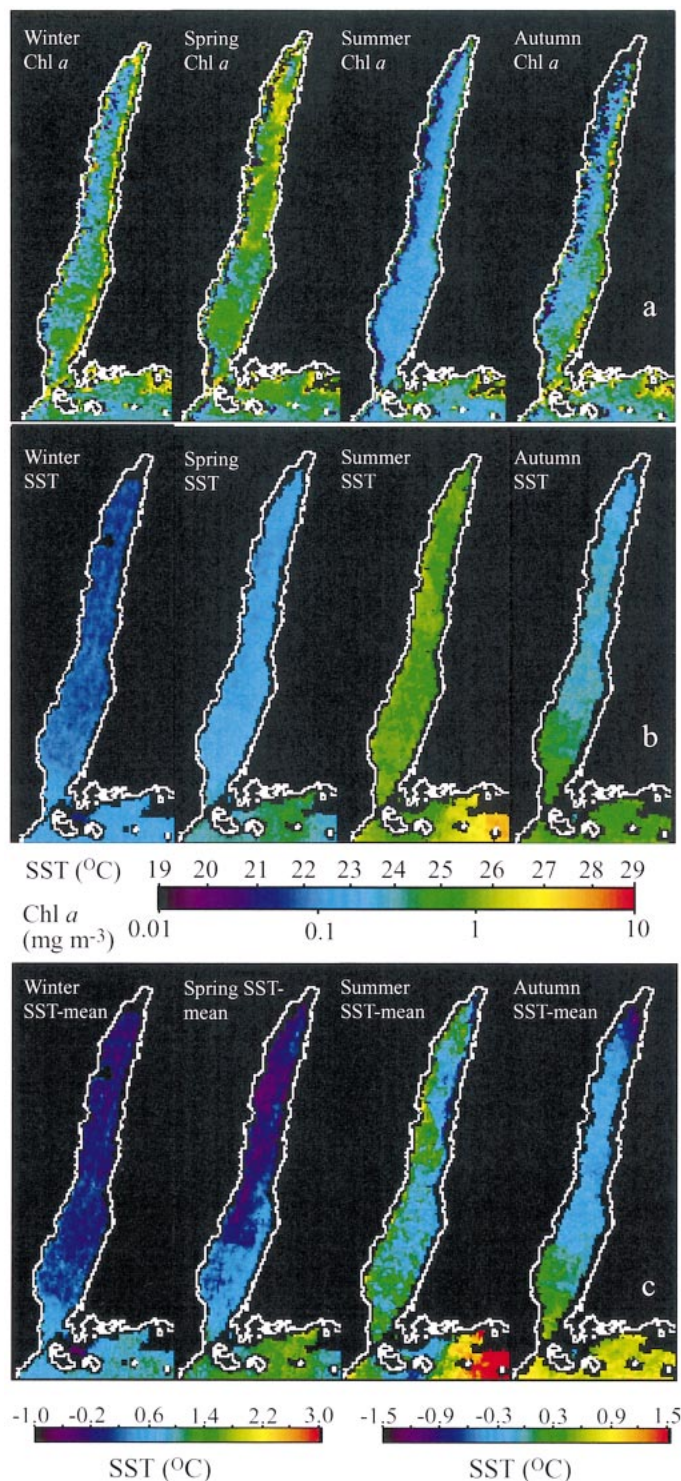


Fig. 3. Seasonal cycles in Chl *a* and SST for the Gulf of Aqaba shown as individual SeaWiFS and MODIS images. (a) SeaWiFS Chl *a* in winter, spring, summer, and autumn. (b) MODIS SSTs for winter, spring, summer, and autumn. (c) SSTs remaining after subtraction of the mean for the Gulf of Aqaba from each pixel in the Gulf of Aqaba, shown for winter, spring, summer, and autumn.

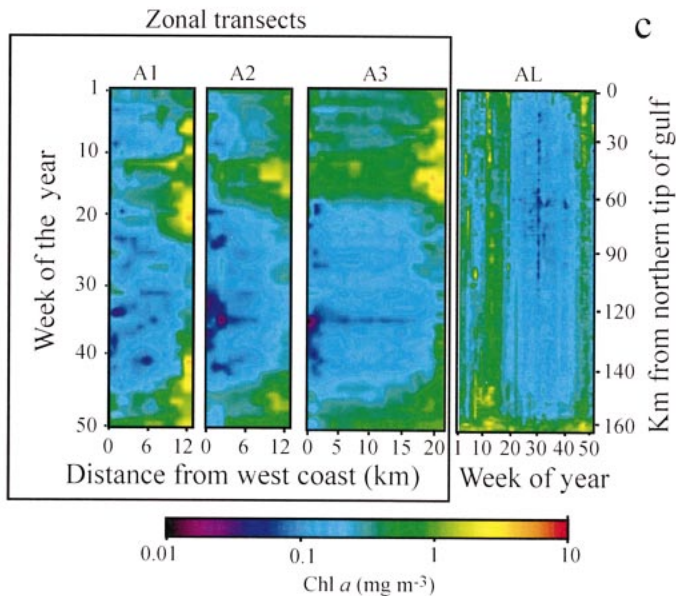
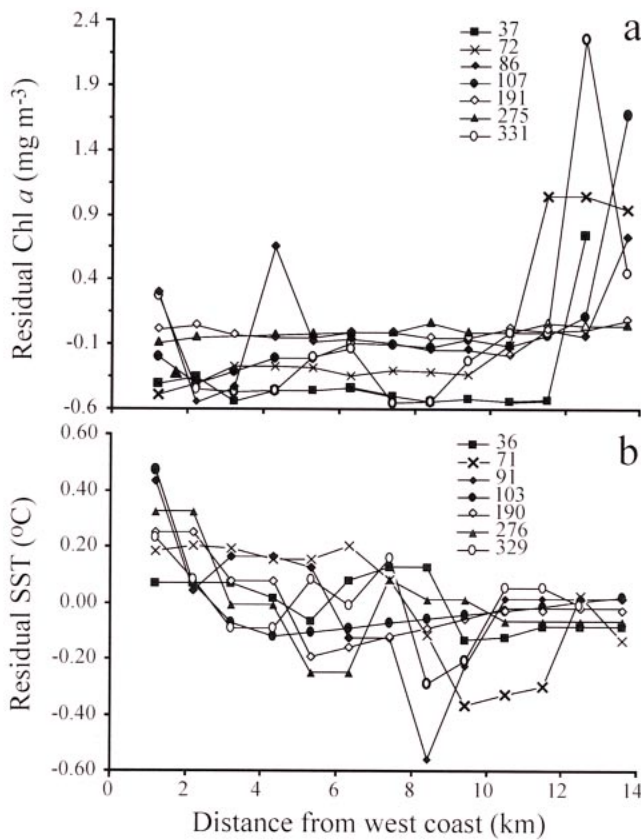


Fig. 4. (a) Gradients in SeaWiFS Chl *a* taken from several transects throughout 1999 (raw data shown). A positive W to E gradient in Chl *a* is seen throughout the year in these transect data. Numbers in legend correspond to the day of the year. (b) Gradients in SeaWiFS SST taken from several transects throughout 2001. Data shown are after subtracting the transect mean from each transect value, and they display a negative W to E gradient throughout the year. Numbers in legend correspond to the day of the year. (c) The annual cycle (3-yr means) showing SeaWiFS Chl *a* in space (horizontal axis) and time (vertical axis) from zonal transects A1, A2,

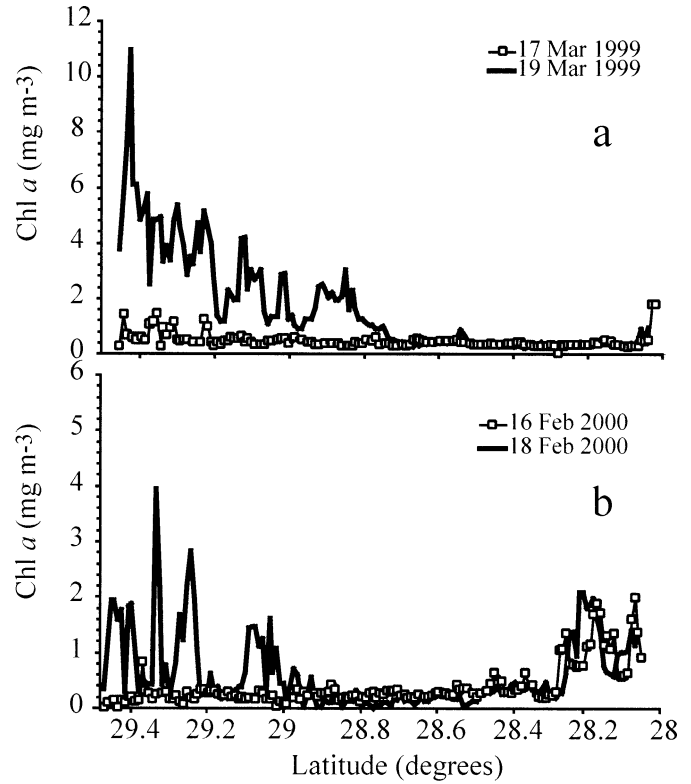


Fig. 5. SeaWiFS data taken from the meridional transect (AL) illustrating the changes in Chl *a* possible during 2-d periods in the Gulf of Aqaba. Both examples from (a) 1999 and (b) 2000 show changes of >10-fold in Chl *a* at the north and central Gulf of Aqaba. Note that the southern end of the Gulf of Aqaba (~28.02°N) exhibits consistently high levels of Chl *a*.

sisted of multiple shorter peaks (e.g., 2 weeks in 1991, see Fig. 6a, inset). Finally, the timing of the spring blooms varied by as much as 1 month from one year to the next, including a 20-d delay in the onset of the spring bloom between 1991 and 1992 and a 35-d difference between 1997 and 1998.

The annual cycle of SST (Fig. 6b) measured at Eilat is relatively simple, with the coldest SST in winter, reaching a minimum of 20–21°C during March (typically the month when the mixed-layer depth reaches its maximum), warming dramatically during the spring, peaking in summer at 26–28°C, and decreasing again during autumn. The variation around the mean among the 4 yr studied was below ±1°C, and the variability was not significant at the 95% confidence level (ANOVA, $P = 0.20$). Spatial variation in MODIS SST (Fig. 3b,c) is generally small, varying by <0.4°C throughout the Gulf of Aqaba and, similar to Chl *a*, exhibits a pattern indicative of upwelling (negative W to E gradient in SST) (Fig. 4b), albeit not as distinct as the Chl *a* signal (Fig. 4a). The largest spatial variation in SST is induced by the rela-

←

and A3 and in space (vertical axis) and time (horizontal axis) for meridional transect AL. The spring and autumn blooms are readily apparent in this figure.

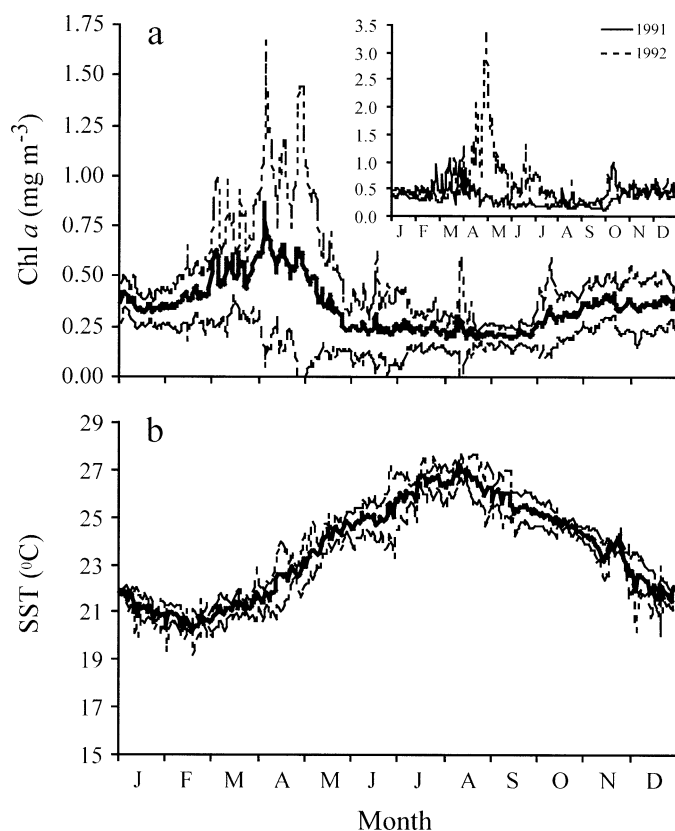


Fig. 6. (a) Mean Chl *a*, 1988–2000, from Eilat, Israel (solid line), flanked by 1 standard deviation (dotted lines). Inset, 1991 and 1992 data showing 1 yr with a typical spring bloom (1991) and 1 yr with an anomalously large spring bloom. (b) Mean SST, 1997–2000, from Eilat, Israel (solid line), flanked by 1 standard deviation (dotted lines).

tively warm water from the Red Sea that enters the southern region of the Gulf of Aqaba and migrates up the east coast during spring and autumn (Fig. 3b). This can be seen most clearly in images where the mean SST for the entire image was subtracted from each image pixel (Fig. 3c).

Interannual variability—The remotely sensed Chl *a* data shown in Fig. 7a–c all demonstrate prominent spring blooms followed by periods of relatively low Chl *a* in the summer, leading to moderately high autumn blooms. However, the duration, onset, and intensity of the blooms varied from year to year. Whereas the spring bloom in 1999 lasted an average of 3 weeks, during 2000 and 2001, it lasted an average of 5 weeks. In terms of the onset of the bloom, the 1999 and 2001 spring blooms began in week 10, whereas the 2000 bloom started a few weeks later in the year. Unlike the 1999 bloom, the 2001 bloom appeared to diminish in intensity and then start again, as indicated by transects A1 and A3. The 1999 seasonally averaged spring Chl *a* was the lowest of the 3 yr at all of the transects, at 0.40 mg Chl *a* m⁻³, whereas 2001 had the highest Chl *a*, averaging 0.58 mg Chl *a* m⁻³, and 2000 was intermediate between the two (0.53 mg Chl *a* m⁻³). During the summer months, Chl *a* was somewhat higher in 2000 than in 1999 and 2001 at all of the transects,

averaging 0.37, 0.13, and 0.21 mg Chl *a* m⁻³, respectively. The autumn bloom was much more distinct in 2000 and 2001, when Chl *a* increased to >0.5 mg m⁻³ in October and remained high throughout the winter months.

There were also differences in the timing and extent of the blooms in the northern end of the Gulf of Aqaba compared to the south. For the 3 yr studied, the seasonal cycle is readily apparent in the satellite data, with the blooms typically being seen first at the southern or mid-Gulf of Aqaba and extending northward. However, the blooms often became more intense in the northern Gulf of Aqaba than in the mid-Gulf or southern Gulf, with 1999 maximum levels (>2 mg Chl *a* m⁻³) being twice as high at A1 as at A2. At the southern end of the Gulf of Aqaba, Chl *a* remained consistently high throughout the year, typically reaching ~1.0 mg Chl *a* m⁻³.

The dominant characteristic of MODIS SST is the seasonal cycle in the Gulf of Aqaba, shown also in the Eilat in situ temperature data (Fig. 6b). The spring bloom began just after the SST started to increase in the late spring (March), associated with the onset of stratification in the Gulf of Aqaba (Fig. 7a–c). The pattern of SST shown in the AL transect follows the typical seasonal cycle of the Eilat SST, but it also shows that the southern region of the Gulf of Aqaba is relatively warmer than the northern/central region during all seasons of the year and that the onset of cooling in late winter is earlier in the northern-to-central Gulf of Aqaba than in the southern Gulf of Aqaba by 2–3 weeks. In fact, warm plumes extended northward from winter to spring from the area of the Straits of Tiran, with a temporally narrower band of cold SST during the winter (spanning weeks 5–10 in the south, compared to weeks 1–20 in the north) (Fig. 7c).

Convection and upwelling dynamics—Evidence from remotely sensed Chl *a* and SST data shows that upwelling is a common occurrence in the Gulf of Aqaba. By examining the transects A1, A2, and A3 (Fig. 7a,b), a pattern emerges that shows consistently higher than average Chl *a* on the eastern side of the Gulf of Aqaba during 1999–2001 (increasing W to E), with correspondingly cooler SSTs on the eastern side of the Gulf of Aqaba (decreasing W to E) during the only year for which such data are available (2001). The upwelling signal, as seen in the zonal transects A1, A2, and A3, is ubiquitous throughout the year. Positive W to E Chl *a* gradients, indicative of upwelling, were strongest during the spring bloom period, persisted into summer, and were still present during the autumn bloom. It can be seen (Fig. 4a) that within a 3-km band closest to the eastern shore of the Gulf of Aqaba, Chl *a* levels were higher than average throughout 2001, although these levels are quite variable. Chl *a* concentrations decreased toward the western side of the Gulf of Aqaba, exhibiting values well below average. The corresponding SST transects exhibit an opposite, albeit weaker signal, with the westernmost 2 km showing SST levels above average, while the middle and eastern Gulf of Aqaba exhibit SSTs at average or well below average in some cases. However, at times, the negative W to E gradient in SST was quite strong, reaching 0.08–0.16°C km⁻¹ (e.g., week 10).

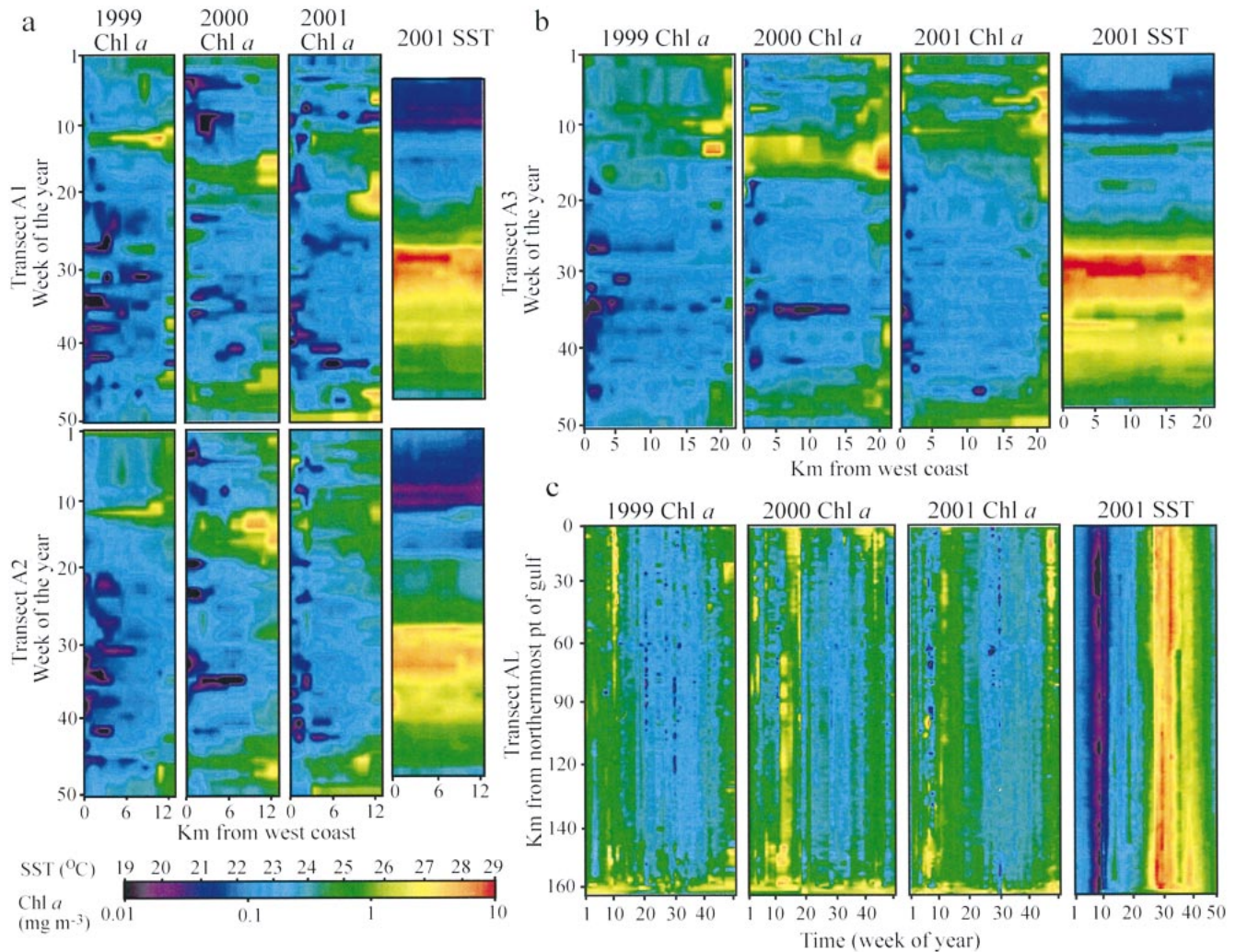


Fig. 7. (a) Plots of weekly-averaged Chl *a* from SeaWiFS (1999–2001) and SST from MODIS (2001) shown in space (horizontal axis) and time (vertical axis) for the northernmost (A1) and middle (A2) zonal transects. (b) Plots of weekly-averaged Chl *a* from SeaWiFS and SST from MODIS for the southernmost zonal transect, A3. (c) Plots of weekly-averaged Chl *a* from SeaWiFS and SST from MODIS for the meridional transect, AL, with time on the horizontal axis and distance on the vertical axis.

Wind patterns in the Gulf of Aqaba are relatively consistent from one year to the next, with the strongest winds occurring in the summer months and blowing from a northerly direction for >90% of the year (Fig. 8a,b). Maximum wind speeds reached 9.49 and 9.25 m s^{-1} during 1999 and 2000, respectively. In 1999, winds were somewhat stronger during the spring and autumn than in 2000, and they dipped lower in the summer of 1999 than in 2000. However, an analysis of variance conducted on mean weekly wind speeds for the 2 yr showed that the 2 yr were not significantly different. The calculated Ekman drift data on the basis of the wind data (optimal longshore upwelling of 15°) are slightly greater in 2000 than in 2001 (Fig. 9) and are consistent with the wind speed data. In 1999, the seasonally integrated Ekman drift was lowest in winter ($1.68 \times 10^6 \text{ m}^{-2}$), which increased to a maximum in spring ($2.50 \times 10^6 \text{ m}^{-2}$) and then remained relatively high during summer and autumn ($2.11 \times 10^6 \text{ m}^{-2}$ and $2.19 \times 10^6 \text{ m}^{-2}$, respectively). In 2000, the Ekman drift was lowest in winter and autumn (1.76×10^6

m^{-2} and $1.71 \times 10^6 \text{ m}^{-2}$, respectively), with the highest values in spring and summer ($2.53 \times 10^6 \text{ m}^{-2}$ and $3.01 \times 10^6 \text{ m}^{-2}$, respectively). The seasonal wind and Ekman drift data are summarized in Table 1. Previous work has shown that wind direction is approximately uniform along the length of the Gulf of Aqaba (Berman et al. 2000), although wind intensity increases slightly toward the southern end.

Heat losses vary more throughout the year. For example, a detailed calculation of the heat fluxes from Eq. 2 (calculated for 1999–2001 from meteorological data) shows values of net cooling that vary between 250 and 400 W m^{-2} (Monismith et al. unpubl. data), with the largest cooling rates in winter. Once heating by shortwave radiation is included, the total rate of cooling is ca. 150 W m^{-2} in winter. Temporal variations in mixed-layer temperature difference are more pronounced, ranging from a maximum of approximately 4°C in September to a few tenths of a degree in March (Paldor and Anati 1979). For the sake of comparison, we assumed a total net heat flux of 150 W m^{-2} (appropriate for December

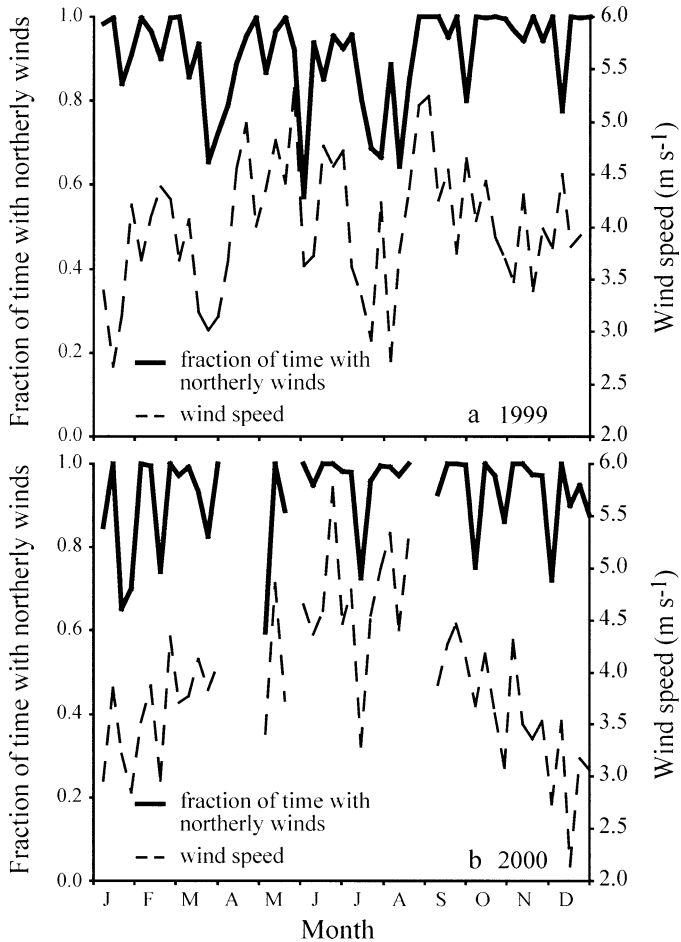


Fig. 8. Weekly averaged winds in the Gulf of Aqaba for (a) 1999 and (b) 2000, showing both the percentage of time that winds are from the north (-45° to 45°) and the mean wind speeds.

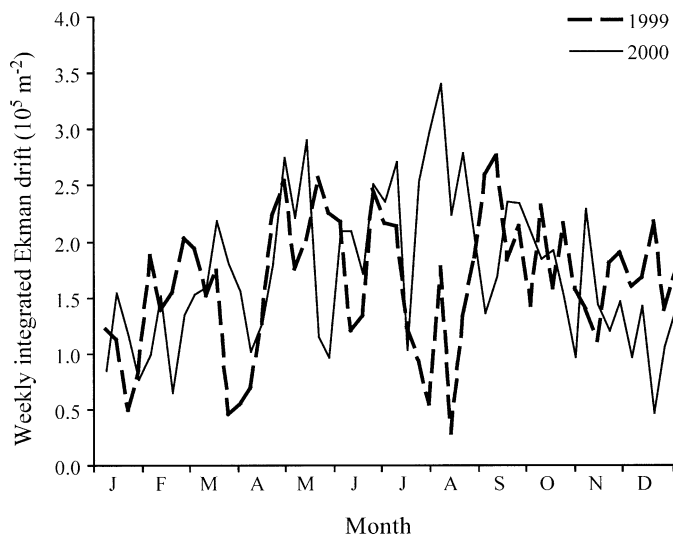


Fig. 9. Weekly integrated upwelling fluxes based on wind fields collected at Eilat, Israel. The fluxes are comparable for both years shown, 1999 and 2000, although they are more similar during winter than during other times of the year.

Table 1. Parameters important in estimating the strength of upwelling in the Gulf of Aqaba, including wind direction (as a percentage of time from the north, the upwelling important direction for the east coast); wind speed (the speed at 10 m above sea level); and Ekman drift.

Season	Mean time winds from north (%)	Mean wind speed (m s^{-1})	Ekman drift (m^{-2} integrated)
1999			
Winter	93	3.64	1.68×10^6
Spring	88	4.28	2.50×10^6
Summer	87	4.04	2.11×10^6
Autumn	95	3.97	2.19×10^6
2000			
Winter	89	3.60	1.76×10^6
Spring	91	4.33	2.53×10^6
Summer	96	4.46	3.01×10^6
Autumn	93	3.35	1.71×10^6

2000–March 2001) and used values of ΔT determined from monthly CTD casts made at Sta. A. Using these data, a comparison of calculated upwelling and entrainment fluxes shows that although upwelling remains relatively constant in time ($\sim 0.2 \text{ m}^2 \text{ s}^{-1}$), convective entrainment varies seasonally, largely in response to changes in the surface-to-bottom temperature contrast (Fig. 10). During early winter, convective entrainment was generally small ($0.15 \text{ m}^2 \text{ s}^{-1}$), but by midwinter, the flows into the mixed layer by convection and upwelling were comparable. By early March, convective entrainment was stronger than upwelling, reaching a value of $0.7 \text{ m}^2 \text{ s}^{-1}$. The net entrainment due to convection was much less in summer and autumn than in early December (data

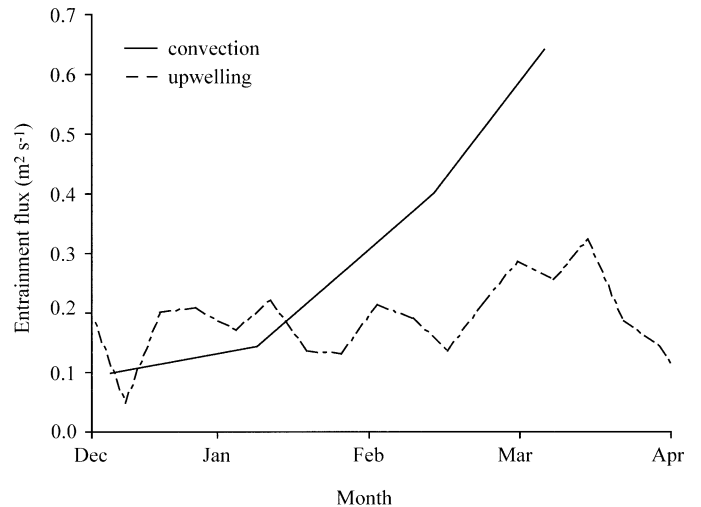


Fig. 10. Entrainment comparison for Gulf of Aqaba Sta. A (near Eilat). Calculated entrainment by upwelling compared to that of convection for 2001. Upwelling is greater than or equal to convection at all times except for late winter/early spring. The calculations are based on a net heat loss of 150 W m^{-2} deduced from change in heat content of Sta. A temp profiles from December 2000 to March 2001. From December to February, the net change in salt content implies an evaporation rate of 1.1 cm d^{-1} .

not shown), and ΔT is larger because the upper water column stratification is strongest at that time (upwelling outweighs convection) (Wolf-Vecht et al. 1992; Genin et al. 1995; Lindell and Post 1995).

Discussion

Seasonal cycle—The Gulf of Aqaba differs from other classic oligotrophic sites (e.g., the Sargasso Sea, oligotrophic North Pacific, Mediterranean Sea), with the strength, timing, and length of phytoplankton blooms and weak stratification being unique characteristics of the Gulf. For example, during a 9-yr time series taken in the Sargasso Sea, the annual cycle included a spring bloom driven by convective winter mixing (DuRand et al. 2001; Steinberg et al. 2001), but unlike in the Gulf of Aqaba, the bloom in the Sargasso Sea peaked at a much lower level of Chl *a*, never reaching $>1 \text{ mg m}^{-3}$ (Steinberg et al. 2001).

During the Atlantic Meridional Transect survey of the oligotrophic Atlantic, the temporal and interannual variability in phytoplankton Chl *a* was very low (typically less than a factor of two) during a 3-yr period (Marañon et al. 2000), whereas phytoplankton Chl *a* in the Gulf of Aqaba can vary by more than two orders of magnitude. In addition, depth-integrated Chl *a* ranged from 20 to 40 mg m^{-2} in the oligotrophic Atlantic, while a conservative estimate for the average integrated Chl *a* during the spring bloom in the Gulf of Aqaba (mixed layer of 100 m) would be closer to 200 mg m^{-2} . Therefore, the Gulf of Aqaba appears to have significantly different phytoplankton biomass dynamics than the oligotrophic Atlantic.

The time series of phytoplankton biomass at the Hawaii Ocean Time Series (HOT) Sta. ALOHA also differs from the Gulf of Aqaba. The average spring levels of Chl *a* were $0.07 \pm 0.02 \text{ mg m}^{-3}$, much lower than those at Eilat ($0.40 \pm 0.36 \text{ mg m}^{-3}$). Summer levels at ALOHA were considerably lower than in the Gulf of Aqaba as well, averaging $0.09 \pm 0.02 \text{ mg Chl } a \text{ m}^{-3}$ compared to the $0.22 \pm 0.09 \text{ mg Chl } a \text{ m}^{-3}$ at Eilat.

The oligotrophic region expected to be most comparable to the Gulf of Aqaba is the Mediterranean Sea, as both are marginal seas bounded at their connections to the open ocean by shallow sills (although the Mediterranean is slightly deeper, 1,500 m average, 5,000 m maximum, and has a larger area than the Gulf of Aqaba). Both seas are characterized by a convectively driven spring phytoplankton bloom, although the strength and timing of the blooms differ between the two seas. For example, during the 9-yr Joint Global Ocean Flux Study DYFAMED cruise in the Mediterranean, depth-integrated Chl *a* levels ranged from below detection during the warm, stratified summers to slightly $>100 \text{ mg m}^{-2}$ during the strongest bloom in spring of 1999 (Marty et al. 2002). In contrast, the northern Gulf of Aqaba exhibited an estimated $>200 \text{ mg Chl } a \text{ m}^{-2}$ during all the spring blooms between 1989 and 2001. In addition, the central Mediterranean Sea exhibits a relatively shallow mixed layer prior to stratification in the spring, typically mixing to $\sim 100 \text{ m}$ (Marty et al. 2002), while in the Gulf of Aqaba, typical winter mixed layers are 250 m with extremes of $>850 \text{ m}$ (Genin

et al. 1995). Finally, unlike the regularity of the autumn blooms in the Gulf of Aqaba, no autumnal blooms were reported during the DYFAMED study, although one such bloom was described by Morel and Andre (1991). On the other hand, results of a numerical model suggest that convective mixing in the eastern oligotrophic Mediterranean Sea is more comparable to that of the Gulf of Aqaba (Napolitano et al. 2000). In addition, Marty et al. (2002) indicate that the strength and duration of the wind plays a relatively large role in the intensity of blooms in the central Mediterranean Sea, and we have found in this study that wind mixing likely plays a larger role in phytoplankton dynamics in the Gulf of Aqaba than was once thought.

Another marginal sea that is comparable to the Gulf of Aqaba is the Sea of Cortez (Gulf of California). This sea is also a rifting basin, and although the northern half is quite shallow due to infilling with sediment from the Colorado River, the depth profile of the southern half is on average 200 m, reaching a maximum on the order of 2,000 m, similar to the Gulf of Aqaba. In addition, upwelling along the eastern shore is prominent in satellite ocean color data of the region (Pegau et al. 2002) and results in high-nutrient input to the surface waters, supporting enhanced biological activity. However, the Sea of Cortez also has an area approximately 10 times larger than the Gulf of Aqaba and is known to be a highly productive coastal region (Alvarez-Borrego 1983) stemming from the strong upwelling flux. The waters entering the Sea of Cortez from the Pacific Ocean are dissimilar to those of the Mediterranean and the Gulf of Aqaba in that they are not restricted to the uppermost, warm, nutrient-poor surface waters and are instead relatively high in nutrients. Therefore, although the Gulf of Aqaba and Sea of Cortez may seem comparable in structure and hydrodynamics, the chemical characteristics and biological dynamics of the two systems are quite dissimilar.

The Chl *a* data gathered in situ from Eilat and obtained from SeaWiFS show that the Gulf of Aqaba exhibits multiple trophic attributes, despite its description as an oligotrophic sea in previous publications (e.g., Levanon-Spanier et al. 1979; Reiss and Hottinger 1984). Chl *a* levels in the Gulf of Aqaba can increase by more than two orders of magnitude within 48 h and are easily more than twofold higher than those of other oligotrophic regions such as HOT, Sargasso, and Mediterranean Seas, even during the summer months (Letelier et al. 1996; Marañon et al. 2000; Ondrusek et al. 2001; Steinberg et al. 2001). In fact, during the spring and autumn blooms, the Gulf of Aqaba is typically eutrophic ($>1.0 \text{ mg Chl } a \text{ m}^{-3}$ as defined by Antoine et al. 1996; Behrenfeld and Falkowski 1997). However, despite such high Chl *a*, the Gulf of Aqaba is dominated by small phytoplankton (primarily *Synechococcus* and *Prochlorococcus*) for much of the year, and nutrients are typically below detection at least for some of the year (Reiss and Hottinger 1984; Lindell and Post 1995) similar to classic oligotrophic regions (e.g., Chisholm et al. 1992; Campbell and Vaultot 1993; Steinberg et al. 2001). The Gulf of Aqaba may be more accurately described as an oligotrophic sea along the western (downwelling) side, while the eastern (upwelling) margin is mesotrophic to eutrophic during much of the year.

The nature of the seasonal phytoplankton dynamics may

have important implications for trophic interactions within the Gulf of Aqaba. First, the abrupt character of the blooms will have consequences for the food web, realized as a stronger decoupling between phytoplankton and zooplankton dynamics (Tagliabue and Arrigo 2003). Second, it has recently been shown that the productive coral reefs in the Gulf of Aqaba subsist to a large degree on allochthonous plankton (Korpál et al. 1992; Yahel et al. 1998; Richter et al. 2001), with N fluxes from the phytoplankton to the reef being 3–20 times greater than other allochthonous sources (Richter et al. 2001). In the absence of a significant spring bloom, phytoplankton may become too scarce to support the large amount of coral reef production found in the Gulf of Aqaba. Therefore, the interannual variability in the strength and timing of phytoplankton blooms may have serious consequences for the upper trophic levels in the Gulf of Aqaba.

Upwelling versus convection—Because the Gulf of Aqaba is weakly stratified, small perturbations such as transient cooling (that induces convection) and wind events (that drive upwelling) can at times mix deep water to the surface euphotic layer, making nutrients available for phytoplankton growth. However, when mixing exceeds the critical depth (Sverdrup 1953), a phytoplankton bloom cannot develop. These opposing consequences of weak stratification may be responsible for the multi-peaked nature of the blooms (Fig. 6a) and the associated rapid changes in Chl *a* (Fig. 5) characteristic of the Gulf of Aqaba. The ubiquitous W to E gradients in Chl *a* and SST throughout the Gulf of Aqaba and the calculated entrainment by upwelling and convection indicate that blooms are controlled in part by upwelling dynamics. It is particularly surprising that the upwelling signal is present during the winter when convective mixing is at its strongest and would be expected to mask any evidence of upwelling (higher Chl *a* on the eastern side of the Gulf of Aqaba, decreasing toward the west). To understand the relative importance of these two processes in controlling phytoplankton blooms in the Gulf of Aqaba, we have developed a conceptual model of the seasonal interplay between convection and upwelling and how these processes influence the spatial and temporal patterns observed in Chl *a* and SST (Fig. 11).

During winter and early spring (from November to early March, Fig. 11), the convective component of entrainment is strong enough to mix the surface waters below the critical depth as well as to bring large quantities of nutrients to the surface. On the eastern side of the Gulf of Aqaba, upwelling counteracts convection, and the mixed-layer depth remains shallower, thus maintaining phytoplankton above the critical depth, resulting in higher growth rates and accumulation of Chl *a*. On the western side, downwelling and convection act in concert to mix phytoplankton below the critical depth, and thus, despite high nutrient fluxes to the surface, the low average light level reduces phytoplankton growth. Therefore, in winter, upwelling in the Gulf of Aqaba is not an important mechanism for providing nutrients to the surface waters, but rather, upwelling acts to modulate mixed-layer deepening and thus prevent phytoplankton cells from circulating below the critical depth. Because the temperature contrast between shallow and deep waters is weak in winter, the E to W dif-

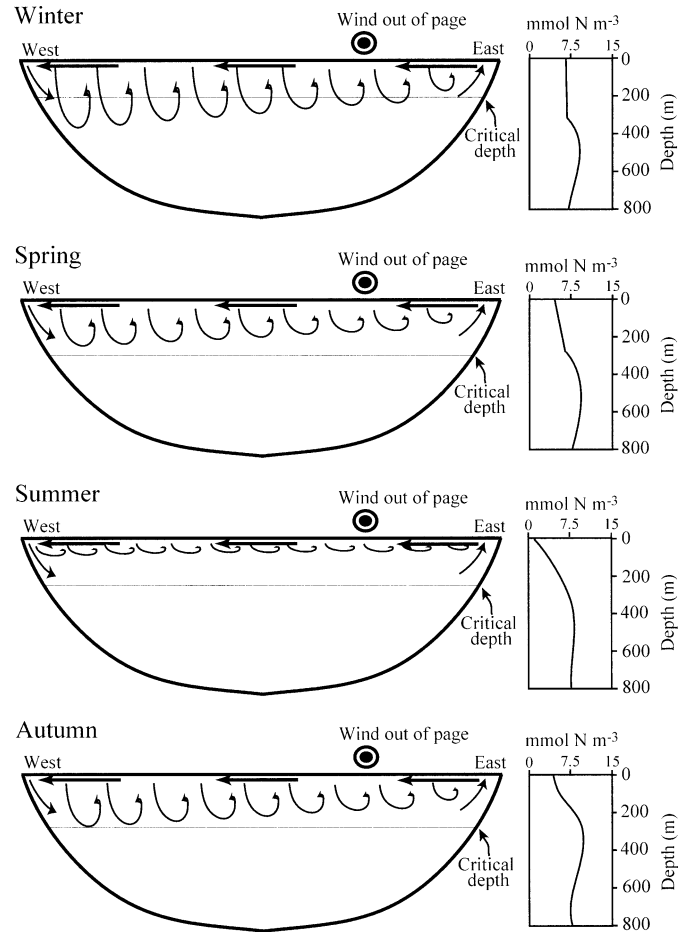


Fig. 11. Schematic of the Gulf of Aqaba showcasing the theorized interplay between upwelling and convection in the Gulf of Aqaba. Winter: shallow critical depth combined with deep convective mixing, offset by upwelling on the east and enhanced by downwelling in the west. Spring: critical depth deepens, and convective mixing decreases in magnitude, allowing blooms to form, with upwelling still present. Summer: deep critical depth is combined with little convective mixing; mixed-layer depth is primarily controlled by wind mixing, and upwelling acts to bring nutrients to the surface and enhance Chl *a* along the eastern side of the Gulf of Aqaba, decreasing toward the west. Autumn: critical depth begins to decrease in depth as the convective mixing starts up; as in winter, upwelling also assists in keeping phytoplankton above the critical depth, but the bloom is not as strong as in the winter because nutrients are not as plentiful during the autumn (mixing has not reached the most nutrient-rich deep waters).

ference in SST due to the upwelling is minute and is irresolvable in MODIS data. An idealized winter N profile shows the upper mixed layer as a homogeneous 250-m layer, with N concentrations increasing slightly at depth (shown as a profile in Fig. 11). These dynamics explain why Chl *a* is higher along the east coast under conditions where both nutrient concentrations and light are relatively high and apparently not limiting in both the east and west sections of the Gulf of Aqaba.

In late spring (mid-March to May, Fig. 11), the critical depth increases due to increased solar insolation and the

mixed-layer shoals somewhat due to thermal stratification, allowing phytoplankton to remain above the critical depth and to bloom throughout the Gulf of Aqaba. This is particularly true in the east, where upwelling can offset the tendency of transient convection events to mix phytoplankton below the critical depth. Presumed N concentrations are somewhat depleted at the surface, increasing at depth to $\sim 7.5 \text{ mmol m}^{-3}$. This scenario results in blooms that develop first on the eastern side of the Gulf of Aqaba and then propagate across the Gulf toward the west as the stratification intensifies.

In summer (from June to September, Fig. 11), the critical depth deepens slightly, and the mixed layer shallows even further (20–30 m depending on wind mixing); at this time, the phytoplankton blooms become controlled by nutrient availability rather than light. In this weakly stratified water column, there is a well-defined nutricline, with N decreasing below detection in the uppermost waters and remaining at 7.5 mmol m^{-3} at 600 m. During this season, upwelling brings nutrients to the surface on the eastern side of the Gulf of Aqaba, resulting in an increase in Chl *a* in the east, which decreases toward the west. During this season, the SST shows a relatively strong upwelling signature, as one would expect given the relatively higher winds during summer. However, the waters of the Gulf of Aqaba are so weakly stratified that the upwelling signature is not clearly evident in the SST data.

In autumn (from September to November, Fig. 11), light is still relatively high, and convective mixing begins, replenishing nutrients in the surface waters. Because the Gulf of Aqaba is weakly stratified, mixing is deep (near the critical depth) but not as deep as during the winter. Therefore, the mixed-layer concentrations of N are moderate, approximately 4 mmol m^{-3} . Upwelling on the east side of the Gulf of Aqaba increases N and decreases SST during the start of the bloom and increases light availability during the end of the bloom. Therefore, the autumn bloom is typically weaker than the spring bloom, exhibits higher Chl *a* in the east than in the west, and is controlled by nutrient availability at the start of the bloom and by light availability at the end, as solar insolation declines and convective mixing increases.

Our conceptual model explains much of the spatial variability in satellite Chl *a* found in this study and is consistent with what is already known about the hydrodynamics in the Gulf of Aqaba. It demonstrates that upwelling and convection can either support or oppose each other, thereby jointly controlling mixed-layer depth and the development of phytoplankton blooms. Our model also relies on the presence of weak thermal stratification in the Gulf of Aqaba, a characteristic that has been described before (e.g., Reiss and Hottinger 1984; Wolf-Vecht et al. 1992; Genin et al. 1995). In this way, the conceptual model accounts for both persistent (i.e., upwelling) and seasonal features (i.e., spring and autumn blooms) and is flexible enough to describe transient changes in Chl *a*, such as those derived from summer wind mixing.

The conceptual model does not include possible additions of nutrients to the surface waters because of remineralization by heterotrophs during autumn or N fixation by diazotrophs during summer months after the spring bloom develops. It

also excludes zooplankton grazing as a controlling factor of phytoplankton biomass. First, although zooplankton produce ammonium that can support a secondary phytoplankton peak in temperate-stratified regions during late summer and autumn (Banse 1995), Chl *a* cannot accumulate to the degree observed in the SeaWiFS data while growing on recycled nutrients. Second, the amount of N fixation in the Gulf of Aqaba has not yet been quantified and cannot be included in this model. Although N fixation provides a source of new N to surface waters, particularly during the summer months (e.g., Capone et al. 1997; Post et al. 2002), rates of N fixation are thought to be lower in subtropical seas than in tropical oligotrophic seas (Capone et al. 1997). However, primary production by *Trichodesmium* is most significant during the summer months, constituting 13–45% of total surface primary production during this season (Post et al. 2002); therefore, its N fixation potential should be included during the summer simulations in future modeling efforts. Finally, for zooplankton grazing to explain the observed positive W to E gradient in Chl *a*, grazing would have to be higher along the western margin. The opposite has been shown to be true, with zooplankton concentrations higher on the eastern side of the Gulf of Aqaba than on the west (Genin et al. unpubl. data). In support of this argument, the Gulf of Aqaba has been described previously as a “bottom-up” (nutrient controlled) rather than a “top-down” (grazing controlled) system (Sommer 2000).

Straits of Tiran—The phytoplankton dynamics in the southern tip of the Gulf of Aqaba do not strictly follow the conceptual model outlined above. This should not be surprising, however, given the role of the sill at the Straits of Tiran. The strong tidal currents and relatively shallow reefs in this area act to turbulently mix nutrients into the surface waters, which are then carried into the Gulf of Aqaba (Murray et al. 1984). Our data show that an omnipresent phytoplankton bloom is located just inside the Straits at the southern tip of the Gulf of Aqaba, likely supported by these nutrients. Relatively low rates of alkaline phosphatase activity near the Straits (Li et al. 1998) also support the hypothesis that nutrients are less limiting in the Straits of Tiran than in other regions of the Gulf throughout much of the year. However, because the nutrient supply to the surface waters in the south is restricted to 250 m of water (moderately high nutrient concentrations) that mixes with nutrient-poor Red Sea water at the Straits, this region does not have access to the deepest, highest-nutrient waters. In contrast, the deeper mixing that typifies the north/central Gulf of Aqaba entrains a higher concentration of nutrients into surface waters. Therefore, the spring bloom in the north/central Gulf of Aqaba is often much larger than the constant bloom in the southern tip of the Gulf, but during the winter and summer months, the levels of Chl *a* in the southern tip of the Gulf are usually higher than those in the north/central Gulf.

The Mediterranean Sea also has a shallow (300 m) sill located at its only connection to the open ocean, the Straits of Gibraltar, and higher production near the Straits has been cited previously (e.g., Estrada 1996; Gomez et al. 2000*a,b*, 2001). Specifically, tidal interactions with the sill are thought to entrain nutrients into the surface waters, which are then

carried into the western Mediterranean Sea by the inflowing Atlantic Ocean waters. These data from the Mediterranean Sea lend support to the hypothesis that the Straits of Tiran and its associated sill also entrain nutrients into the surface water and support phytoplankton growth in the southern Gulf of Aqaba.

Conclusions—The Gulf of Aqaba shares several characteristics with other oligotrophic oceanic regions while simultaneously displaying several unique features. Its annual cycle of phytoplankton biomass is closest to that of a temperate ocean, with both spring and autumn blooms, but the depth of convective mixing displayed in the Gulf of Aqaba is extreme. Therefore, although it is one of the warmest, most nutrient-poor seas during the summer, its weak stratification and upwelling favorable winds allow it to produce more phytoplankton than are typically found in other oligotrophic regions (e.g., the Sargasso Sea, oligotrophic North Pacific, Mediterranean Sea). However, the most common phytoplankton taxa in the Gulf of Aqaba (primarily ultra-phytoplankton) are also dominant in other oligotrophic systems. The conceptual model described in this study captures much of the large-scale phytoplankton bloom dynamics in the Gulf of Aqaba; however, it ignores physical processes such as meridional advection and turbulent mixing as well as biologically driven processes such as trophic interactions, microbial loop activity, and N fixation. In light of the limitations of the conceptual model, our understanding of the phytoplankton dynamics in the Gulf of Aqaba would be further enhanced by a three-dimensional coupled physical and biological model.

References

- ALVAREZ-BORREGO, S. 1983. Gulf of California, p. 427–449. *In* B. H. Ketchum [ed.], *Ecosystems of the world—estuaries and enclosed seas*. Elsevier.
- ANTOINE, D., J. M. ANDRE, AND A. MOREL. 1996. Oceanic primary production: 2. Estimation at global scale from satellite (Coastal Zone Color Scanner) chlorophyll. *Global Biogeochem. Cycles* **10**: 57–69.
- BANSE, K. 1995. Zooplankton: Pivotal role in the control of ocean production. *ICES J. Mar. Sci.* **52**: 265–277.
- BEHRENFELD, M. J., AND P. G. FALKOWSKI. 1997. Photosynthetic rates derived from satellite-based chlorophyll concentration. *Limnol. Oceanogr.* **42**: 1–20.
- BERMAN, T., N. PALDOR, AND S. BRENNER. 2000. Simulation of wind-driven circulation in the Gulf of Elat (Aqaba). *J. Mar. Syst.* **26**: 349–365.
- BLANTON, J. G. 1973. Vertical entrainment into the epilimnion of stratified lakes. *Limnol. Oceanogr.* **18**: 697–701.
- CAMPBELL, L., AND D. VAULOT. 1993. Photosynthetic picoplankton community structure in the subtropical north Pacific Ocean near Hawaii (station ALOHA). *Deep-Sea Res. I* **40**: 2043–2060.
- CAPONE, D. G., J. P. ZEHR, H. W. PAERL, B. BEGMAN, AND E. J. CARPENTER. 1997. *Trichodesmium*, a globally significant marine cyanobacterium. *Nature* **276**: 1221–1229.
- CARLSON, C. A., H. W. DUCKLOW, AND A. F. MICHAELS. 1994. Annual flux of dissolved organic carbon from the euphotic zone in the northwestern Sargasso Sea. *Nature* **371**: 405–408.
- CHISHOLM, S., AND OTHERS. 1992. *Prochlorococcus marinus* nov gen nov sp: An oxyphototrophic marine prokaryote containing divinyl chlorophyll a and chlorophyll b. *Arch. Microbiol.* **157**: 297–300.
- CLAUSTRE, H., AND J. C. MARTY. 1995. Specific phytoplankton biomasses and their relation to primary production in the tropical north Atlantic. *Deep-Sea Res. I* **42**: 1475–1493.
- , AND OTHERS. 2002. Is desert dust making oligotrophic waters greener? *Geophys. Res. Lett.* **29**: 1–4.
- DURAND, M. D., R. J. OLSON, AND S. W. CHISHOLM. 2001. Phytoplankton population dynamics at the Bermuda Atlantic Time-series station in the Sargasso Sea. *Deep-Sea Res. II* **48**: 1983–2003.
- EPPLEY, R. W. 1972. Temperature and phytoplankton growth in the sea. *Fish. Bull.* **70**: 1063–1085.
- ESTRADA, M. 1996. Primary production in the northwestern Mediterranean. *Sci. Mar.* **60**: 55–64.
- GENIN, A., B. LAZAR, AND S. BRENNER. 1995. Vertical mixing and coral death in the Red Sea following the eruption of Mount Pinatubo. *Nature* **377**: 507–510.
- GILL, A. E. 1982. *Atmosphere–ocean dynamics*. Academic Press.
- GOMEZ, F., AND OTHERS. 2000a. Microplankton distribution in the Strait of Gibraltar: Coupling between organisms and hydrodynamic structure. *J. Plankton Res.* **22**: 603–617.
- , N. GONZALEZ, F. ECHEVARRIA, AND C. M. GARCIA. 2000b. Distribution and fluxes of dissolved nutrients in the Strait of Gibraltar and its relationships to microphytoplankton biomass. *Estuarine Coastal Shelf Sci.* **51**: 439–449.
- , AND OTHERS. 2001. Small-scale temporal variations in biogeochemical features in the Strait of Gibraltar, Mediterranean side: The role of NACW and the interface oscillation. *J. Mar. Syst.* **30**: 207–220.
- KLINKER, J., Z. REISS, C. KROPACH, I. LEVANON, H. HARPAZ, AND Y. SHAPIRO. 1978. Nutrients and biomass distribution in the gulf of Aqaba (Elat), Red Sea. *Mar. Biol.* **45**: 53–64.
- KORPAL, T., B. LAZAR, AND J. EREZ. 1992. Fluxes of material and energy between coral reefs and the open sea. *Environ. Sci. Res.* **43**: 517.
- LETELIER, R. M., J. E. DORE, C. D. WINN, AND D. M. KARL. 1996. Seasonal and interannual variations in photosynthetic carbon assimilation at Station ALOHA. *Deep-Sea Res. II* **43**: 467–490.
- LEVANON-SPANIER, I., E. PADAN, AND Z. REISS. 1979. Primary production in a desert-enclosed sea: The Gulf of Elat (Aqaba), Red Sea. *Deep-Sea Res. I* **26**: 673–686.
- LI, H., M. J. W. VELDHUIS, AND A. F. POST. 1998. Alkaline phosphatase activities among planktonic communities in the northern Red Sea. *Mar. Ecol. Prog. Ser.* **173**: 107–115.
- LINDELL, D., AND A. F. POST. 1995. Ultraphytoplankton succession is triggered by deep winter mixing in the Gulf of Aqaba (Eilat), Red Sea. *Limnol. Oceanogr.* **40**: 1130–1141.
- MARAÑON, E., P. M. HOLLIGAN, M. VARELA, B. MOURIÑO, AND A. J. BALE. 2000. Basin-scale variability of phytoplankton biomass, production and growth in the Atlantic Ocean. *Deep-Sea Res. I* **47**: 825–857.
- MARTY, J., J. CHIAVERINI, M. PIZAY, AND B. AVRIL. 2002. Seasonal and interannual dynamics of nutrients and phytoplankton pigments in the western Mediterranean Sea at the DYFAMED time-series station (1991–1999). *Deep-Sea Res. II* **49**: 1965–1985.
- MOREL, A., AND J. M. ANDRE. 1991. Pigment distribution and primary production in the western Mediterranean as derived and modeled from Coastal Zone Color Scanner observations. *J. Geophys. Res.* **96**: 12685–12698.
- MURRAY, S. P., A. HECHT, AND A. BABCOCK. 1984. On the mean flow in the Tiran Strait in winter. *J. Mar. Res.* **42**: 265–287.
- NAPOLITANO, E., T. OGUZ, P. MALANOTTE-RIZZOLI, A. YILMAZ, AND

- E. SANSONE. 2000. Simulations of biological production in the Rhodes and Ionian basins of the eastern Mediterranean. *J. Mar. Syst.* **24**: 277–298.
- ONDRUSEK, M. E., R. R. BIDIGARE, S. T. SWEET, D. A. DEFREITAS, AND J. M. BROOKS. 1991. Distribution of phytoplankton pigments in the North Pacific Ocean in relation to physical and optical variability. *Deep-Sea Res. I* **38**: 243–266.
- , ———, K. WATERS, AND D. M. KARL. 2001. A predictive model for estimating rates of primary production in the subtropical North Pacific Ocean. *Deep-Sea Res. II* **48**: 1837–1863.
- PALDOR, N., AND D. A. ANATI. 1979. Seasonal variations of temperature and salinity in the Gulf of Elat (Aqaba). *Deep-Sea Res. I* **26**: 661–672.
- PEGAU, W. S., E. BOSS, AND A. MARTINEZ. 2002. Ocean color observations of eddies during the summer in the Gulf of California. *Geophys. Res. Lett.* **29**: 1–3.
- POST, A. F., AND OTHERS. 2002. Spatial and temporal distributions of *Trichodesmium* spp. in the stratified Gulf of Aqaba, Red Sea. *Mar. Ecol. Prog. Ser.* **239**: 241–250.
- , M. VELDHUIS, AND D. LINDELL. 1996. Spatial and temporal distribution of ultraphytoplankton in the Gulf of Aqaba, Red Sea. *J. Phycol. (suppl.)* **32**: 38–39.
- REISS, Z., AND L. HOTTINGER. 1984. *The Gulf of Aqaba ecological paleontology*. Springer.
- RICHTER, C., M. WUNSCH, M. RASHEED, I. KOTTER, AND M. I. BADRAN. 2001. Endoscopic exploration of Red Sea coral reefs reveals dense populations of cavity-dwelling sponges. *Nature* **413**: 726–730.
- SHERMAN, F. S., J. IMBERGER, AND G. M. CORCOS. 1978. Turbulence and mixing in stably stratified waters. *Annu. Rev. Fluid Mech.* **10**: 267–288.
- SMITH, S. D. 1980. Wind stress and heat flux over the ocean in gale force winds. *J. Phys. Oceanogr.* **10**: 709–726.
- SOMMER, U. 2000. Scarcity of medium-sized phytoplankton in the northern Red Sea explained by strong bottom-up and weak top-down control. *Mar. Ecol. Prog. Ser.* **197**: 19–25.
- , AND OTHERS. 2002. Grazing during early spring in the Gulf of Aqaba and the northern Red Sea. *Mar. Ecol. Prog. Ser.* **239**: 251–261.
- STEINBERG, D. K., C. A. CARLSON, N. R. BATES, R. J. JOHNSON, A. F. MICHAELS, AND A. H. KNAP. 2001. Overview of the US JGOFS Bermuda Atlantic Time-Series Study (BATS): A decade-scale look at ocean biology and biogeochemistry. *Deep-Sea Res. II* **48**: 1405–1447.
- SVERDRUP, H. U. 1953. On conditions for the vernal blooming of phytoplankton. *J. Cons. Perm. Int. Explor. Mer.* **18**: 287–295.
- TAGLIABUE, A., AND K. R. ARRIGO. 2003. Anomalous low zooplankton abundance in the Ross Sea: An alternative explanation. *Limnol. Oceanogr.* **48**: 686–699.
- WOLF-VECHT, A., N. PALDOR, AND S. BRENNER. 1992. Hydrographic indications of advection/convection effects in the Gulf of Elat. *Deep-Sea Res. I* **39**: 1393–1401.
- YAHIEL, G., A. F. POST, K. FABRICIUS, D. MARIE, D. VAULOT, AND A. GENIN. 1998. Phytoplankton distribution and grazing near coral reefs. *Limnol. Oceanogr.* **43**: 551–563.
- ZIMMER, C. 2001. The partitioning of the Red Sea. *Science* **293**: 627–628.

Received: 9 October 2002

Accepted: 26 May 2003

Amended: 25 July 2003